Optical Materials 72 (2017) 644–649

Contents lists available at ScienceDirect

Optical Materials

journal homepage: www.elsevier.com/locate/optmat

Energy transfer mechanism and optoelectronic properties of (PFO/TiO_2)/Fluorol 7GA nanocomposite thin films

Bandar Ali Al-Asbahi [a, b, *]

[a] Department of Physics and Astronomy, College of Science, King Saud University, Saudi Arabia
[b] Department of Physics, Faculty of Science, Sana'a University, Yemen

ARTICLE INFO

Article history:
Received 14 February 2017
Received in revised form
4 July 2017
Accepted 5 July 2017

Keywords:
Energy transfer properties
Förster-type
Donor/acceptor
Optoelectronic properties
OLED

ABSTRACT

Energy transfer between poly (9,9'-di-n-octylfluorenyl-2,7-diyl) (PFO) as a donor in presence of TiO_2 nanoparticles (NPs) and Fluorol 7GA as an acceptor with different weight ratios has been investigated by steady-state emission measurements. Based on the absorption and fluorescence measurements, the energy transfer properties, such as quenching rate constant (k_{SV}), energy transfer rate constant (k_{ET}), quantum yield (ϕ_{DA}), and lifetime (τ_{DA}), of the donor in the presence of the acceptor, energy transfer probability (P_{DA}), energy transfer efficiency (η), energy transfer time (τ_{ET}), and critical distance of the energy transfer (R_o) were calculated. Förster-type energy transfer between the excited donor and ground-state acceptor molecules was the dominant mechanism responsible for the energy transfer as evidenced by large values of k_{SV}, k_{ET}, and R_o. Moreover, these composite materials were employed as an emissive layer in organic light-emitting diodes (OLEDs). Additionally, the optoelectronic properties of OLEDs were investigated in terms of current density–voltage characteristics and electroluminescence spectra.

1. Introduction

Förster resonance energy transfer (FRET) is known as dipole-dipole or through-space energy transfer, and includes long-range coupling of acceptor and donor dipoles. The Förster mechanism is based on resonance between two oscillating dipoles (i.e., electric fields associated with electrons). The two dipoles can be coupled coulombically if the ground state of one molecule and the excited state of a neighboring molecule have matching oscillating electric fields. Consequently, the energy of the excited state can be transferred from a donor to an acceptor through space (without the exchange of electrons). The FRET efficiency depends on the relative orientation of the donor emission dipole moment and the acceptor absorption dipole moment. It reaches a maximum when the transition dipole of the acceptor ground state and oscillating dipole of the excited donor are aligned [1]. FRET occurs if the acceptor absorption spectrum and donor emission spectrum overlap significantly, and the distance between the donor and acceptor is not much greater than the Förster radius (R_0). The Förster radius depends on the dipole orientation and spectral overlap between the acceptor absorption band and donor emission band [2]. FRET plays an important role in the donor-acceptor blending that has been used to achieve high performance efficiency of organic light-emitting diodes (OLEDs) [3–7].

Polyfluorene derivatives are attractive candidates for OLEDs because of their good chemical and thermal stability and their remarkably high solid-state and solution fluorescence quantum yields [8,9]. Furthermore, their properties such as processability, morphology, and solubility can be controlled due to the facile substitution at the 9-position of the fluorene monomer.

The optimization of the luminescence efficiency of OLEDs can be achieved by balancing the electron and hole injection using two different materials with heterogeneous electrical properties [10,11]. In addition, the enhancement of the optical properties of a polymer blend can be accomplished by shifting the emission wavelength away from the absorption band of the dominant polymer to decrease the optical loss. The wavelength shift can be achieved by FRET from the excited state of the donor to the ground state of the acceptor polymer [10,12]. Unfortunately, some problems can arise once the acceptor content exceeds a certain value

* Department of Physics and Astronomy, College of Science, King Saud University, Saudi Arabia.
E-mail addresses: alasbahibandar@gmail.com, balasbahi@ksu.edu.sa.

http://dx.doi.org/10.1016/j.optmat.2017.07.013
0925-3467/

due to the formation of dark quenchers [13]. This can be prevented, and the enhancement of the energy transfer in the system and OLEDs performance can be achieved by several methods such as addition of nanostructure metal oxides like TiO_2 nanoparticles (NPs) [3], side chain approach [14], annealing [15], and dopant control [16].

Poly (9,9'-di-n-octylfluorenyl-2,7-diyl) (PFO)/TiO_2/Fluorol 7GA is one of the most interesting conjugated polymer/TiO_2/dye nanocomposites where the conjugated polymer acts as a donor and dye as an acceptor. In the present work, we report that the strong overlap between the emission spectrum of the donor and absorption spectrum of the acceptor in the presence of TiO_2 NPs is essential for the efficient FRET in the donor/acceptor blend. Despite the important accomplishments in polymer/dye hybrids, there is no in-depth study on the influence of the fixed composition of inorganic nanostructures on the energy transfer parameters in the PFO/Fluorol 7GA hybrid. In our previous work [4], the efficient energy transfer between PFO and Fluorol 7GA was demonstrated. The goal of the present work is a detailed investigation of the energy transfer properties of the PFO/Fluorol 7GA hybrid in the presence of a fixed content of TiO_2 NPs. Furthermore, the influence of TiO_2 NPs on the enhancement of the energy transfer parameters and thus FRET is investigated here in detail. In addition, the optoelectronic properties of the (PFO/TiO_2)/Fluorol 7GA, which is used as a single emitting layer in the OLED, are demonstrated.

2. Experimental procedures

2.1. Materials

The Fluorol 7GA (M_W = 324.41) was obtained from Exciton (Dayton, Ohio, USA). The TiO_2 powder (average size of 25 nm) and poly (9,9'-di-n-octylfluorenyl-2,7-diyl) (PFO) (M_W = 58200) were obtained from Sigma-Aldrich (St. Louis, MO, USA). Toluene solvent produced by Fluka (Buchs, Switzerland) was used to dissolve all of these materials. Both indium tin oxide (ITO) and glass substrates were purchased from Merck Balzers (Balzers, Liechtenstein).

2.2. Thin film preparation

All samples were deposited onto the glass substrates for both absorption and photoluminescence (PL) measurements and onto the ITO substrates for the current density–voltage (J–V) and electroluminescence (EL) measurements. Before OLED fabrication, the ITO substrate, which served as an anode, was first etched and patterned by exposing to vapor of nitrate acid (HNO_3) and hydrochloric acid (HCl) in a molar ratio of 1:3. Then, the ITO substrate was cleaned sequentially in acetone and isopropanol under ultrasonication for 15 min at each step to clean the surface and remove any impurities.

Under sonication for 1 h, different weight ratios of Fluorol 7GA (0.1, 0.3, 0.5, 1.0, 3.0, and 5.0 wt %) were added to a fixed ratio of PFO: TiO_2 (90:10 wt %). For all samples, the concentration of PFO was fixed at 15 mg/ml. Using the spin-coating technique, (PFO: TiO_2)/Fluorol 7GA composites were deposited onto the substrates with dimensions of 2 cm × 1.2 cm. The deposition parameters were fixed at a rotational speed of 2000 rpm for 0.5 min. Then, to remove the solvent from the film, it was baked at 120 °C for 10 min in a vacuum oven. The ITO substrates containing organic film were transferred to an electron beam chamber to deposit an aluminum cathode. The deposition rate was 2 Å/min at a chamber pressure of 2.5×10^{-6} Pa. The thickness and active area of the fabricated aluminum cathode were 150 nm and 0.076 cm^2, respectively.

2.3. Sample characterization

Perkin Elmer Lambda 900 UV–VIS Spectrometer and Perkin Elmer (LS55) Luminescent Spectrophotometer were employed to obtain absorption and PL spectra, respectively. A Keithley 238 measurement system and HR2000 Ocean Optic Spectrometer were used for J–V and EL measurements, respectively.

3. Results and discussion

According to Fig. 1, there is a strong evidence of efficient energy transfer between monomers of the donor (PFO) in the presence of TiO_2 NPs and molecules of the acceptor (Fluorol 7GA) due to a large spectral overlap between the absorption spectrum of Fluorol 7GA and emission spectrum of PFO/TiO_2. Consequently, the Förster-type energy transfer is possible in this system. As a result of strong spectral overlap between absorbance of acceptor and emission of donor, the probability of electron transfer is considered insignificant. The emission spectra shown in Fig. 2 support this conclusion. Moreover, the radiative energy transfer between the donor and acceptor is weak because of low acceptor concentration. These findings are consistent with the previous reported studies in which FRET is the dominant mechanism for energy transfer in most polymer-dye blends [4,17,18].

Fig. 2 also shows that the maximum emission intensities experience a red shift with increasing acceptor concentration. This effect can be attributed to radiative migration due to self-absorption [19,20]. When the Fluorol 7GA concentration exceeded 5 wt%, the emission of PFO in the presence of the TiO_2 NPs was almost entirely quenched, which resulted in complete energy transfer from the donor to the acceptor. This quenching is the evidence of the efficient nonradiative energy transfer between the monomers of PFO in the presence of the TiO_2 NPs and molecules of Fluorol 7GA [21]. The emission intensity from the acceptor had a maximum at 1.0 wt% of Fluorol 7GA in the nanocomposites. Increasing the Fluorol 7GA concentration above 1.0 wt% resulted in decreasing emission intensity. This decrease can be attributed to the aggregation of the Fluorol 7GA molecules [4].

The FRET parameters of the system can be determined from the absorption and fluorescence spectra of the nanocomposites. The Stern–Volmer (k_{SV}) and quenching rate (k_q) constants can be estimated as follows [22,23]:

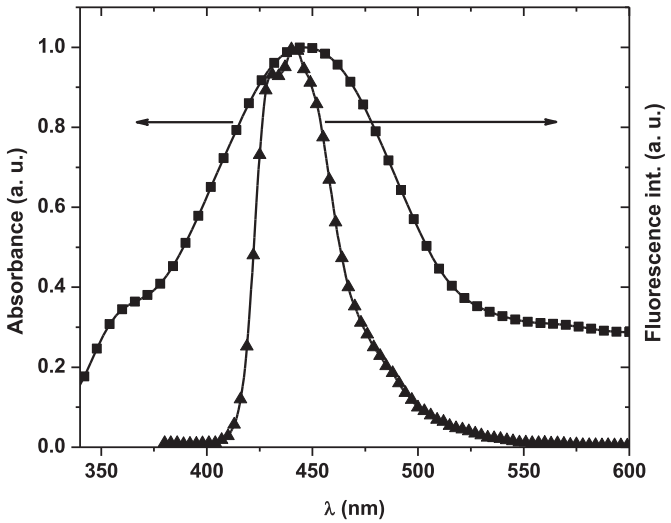

Fig. 1. Absorption spectrum of Fluorol 7GA and emission spectrum of PFO in the presence of TiO_2.

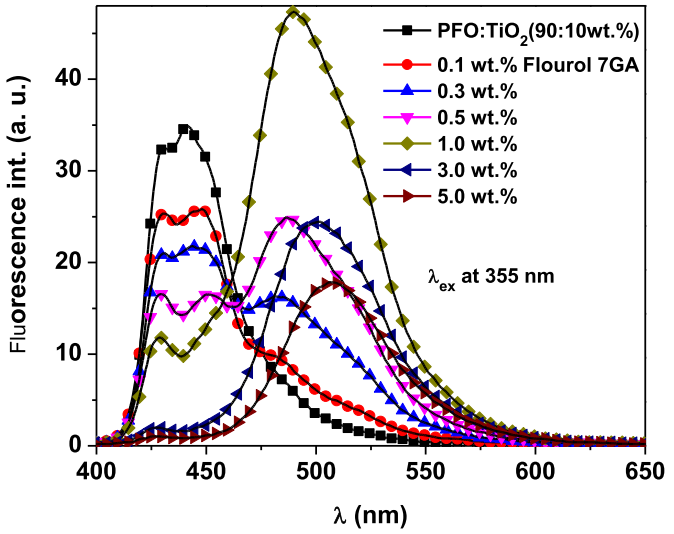

Fig. 2. Emission spectra of PFO/TiO_2 in the absence and presence of Fluorol 7GA at different ratios (λ_{ex} = 355 nm).

$$\frac{I_D}{I_{DA}} = 1 + k_{SV}[A] \tag{1}$$

$$k_q = \frac{k_{SV}}{\tau_D} \tag{2}$$

where I_D and I_{DA} are the fluorescence intensities of the donor in the absence and presence of the acceptor, respectively, [A] is the acceptor concentration, and τ_D (~346 ps) [4] is the excited state lifetime of the donor in the absence of the acceptor. The homogeneity of the dynamic quenching of the PFO by the Fluorol 7GA in the presence of the TiO_2 NPs can be detected from the linear Stern–Volmer plot (Fig. 3). The obtained value of k_{SV} (~0.011 $(\mu M)^{-1}$) suggests that 50% of the fluorescence was quenched at the Fluorol 7GA concentration of almost 90.9 μM (0.029 mg/ml), whereas it was quenched at 50 μM in the absence of TiO_2 NPs [4]. Although the obtained value of k_q (3.12×10^{13} M^{-1} S^{-1}) is less than

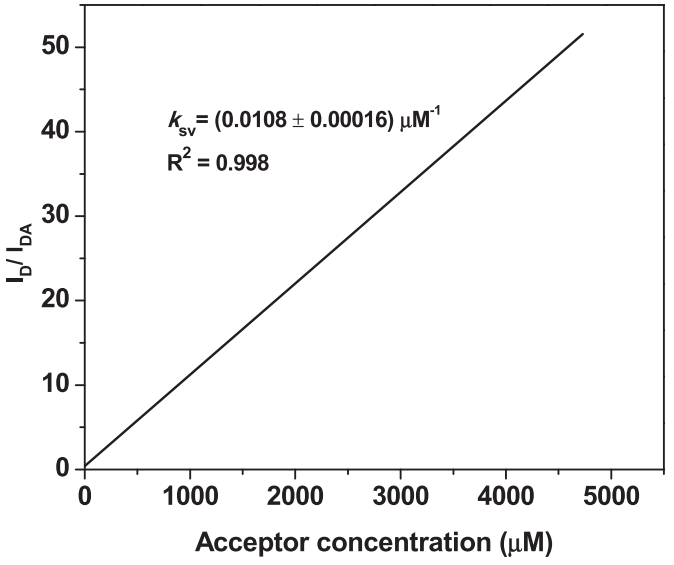

Fig. 3. Stern–Volmer plots for the emission quenching of PFO/TiO_2 by different concentrations of Fluorol 7GA.

that in the absence of TiO_2 NPs [4], it is still significantly greater than 1×10^{10} M^{-1} S^{-1}, which is the minimum value for efficient quenching [24]. Moreover, the high value of k_q is the evidence of the good mixing and thus the excellent quality of the interface between PFO and Fluorol 7GA in the presence of TiO_2 NPs.

Because of the homogeneous dynamic quenching of PFO by Fluorol 7GA in the presence of the TiO_2 NPs, the Stern–Volmer equation can also be represented as:

$$\frac{I_D}{I_{DA}} = \frac{\tau_D}{\tau_{DA}} = \frac{\varnothing_D}{\varnothing_{DA}} \tag{3}$$

where ϕ_D ~ 0.72 [4] is the fluorescence quantum yield of PFO in the absence of Fluorol 7GA, whereas τ_{DA} and φ_{DA} are the excited state lifetime and fluorescence quantum yield of PFO in the presence of Fluorol 7GA, respectively [24]. The τ_{DA} and φ_{DA} values in the presence of TiO_2 NPs for different Fluorol 7GA weight ratios have been calculated and presented in Table 1. It is clear that an increase in the Fluorol 7GA ratio leads to a dramatic decrease in the values of φ_{DA}. This decrease provides additional evidence for the low probability of the radiative energy transfer. Meanwhile, an additional evidence for the FRET efficiency has a significantly lower value of τ_{DA} compared to τ_D in the presence of TiO_2 NPs [25]. The values of τ_{DA} and φ_{DA} with TiO_2 NPs are almost two times smaller than those without TiO_2 NPs [4], which confirms the positive effect of TiO_2 NPs on the enhancement of nonradiative energy transfer from PFO to Fluorol 7GA.

The probability (P_{DA}) and efficiency (η) of the donor-acceptor energy transfer in the presence of TiO_2 NPs were calculated using Eqs. (4) and (5), respectively [26].

$$P_{DA} = \frac{1}{\tau_D}\left(\frac{I_D}{I_{DA} - 1}\right) \tag{4}$$

$$\eta = 1 - \frac{I_{DA}}{I_D} = \frac{R_0^6}{R_{DA}^6 + R_0^6} \tag{5}$$

where R_0 is the Förster transfer radius defined as the intermolecular separation between the acceptor and donor (R_{DA}) at which the Förster energy transfer competes equally with all other de-excitation mechanisms.

An exponential relationship between P_{DA} and acceptor weight ratios can be clearly seen in Fig. 4. The gradual increase in P_{DA} values with addition of Fluorol 7GA resulted from the systematic reduction in the fluorescence intensity (I_{DA}) of the PFO/TiO_2 nanocomposite.

Fig. 5 demonstrates a systematic increase in η with initial addition of the Fluorol 7GA until its content reaches 3 wt%. The maximum energy transfer efficiency is around 97%. This value remains almost unchanged even if the Fluorol 7GA content exceeds 3 wt%. The insignificant variation of η when the acceptor content exceeds 3 wt% can be attributed to the trivial change in the

Table 1
Quantum yield, lifetime of PFO/TiO_2 in the presence Fluorol 7GA and the overlap integral, critical energy transfer distance between the donor/TiO_2 and acceptor.

Acceptor content in (donor/TiO_2)/acceptor blend	ϕ_{DA}	τ_{DA} (ps)	J (λ) × 10^{15} (M^{-1} cm^{-1} nm^4)	R (Å)
0.1 wt %	0.56	269	8.50	60.33
0.3 wt %	0.46	224	8.03	59.76
0.5 wt %	0.37	176	6.25	57.32
1.0 wt %	0.26	126	4.02	53.25
3.0 wt %	0.044	21.2	1.50	45.18
5.0 wt %	0.023	11.1	1.02	42.36

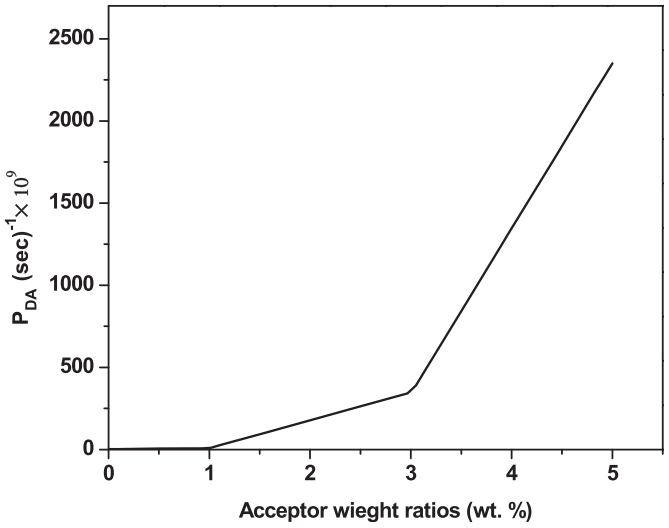

Fig. 4. Probability of energy transfer from PFO/TiO_2 to Fluorol 7GA for different weight ratios.

fluorescence intensity of PFO/TiO_2 nanocomposite, as previously shown in Fig. 2.

The critical transfer distance (*i.e.*, the Förster radius) can be estimated using the following formula [27]:

$$R_o^6 = \frac{9000(\ln 10)\beta^2\phi_D}{128\pi^5 n^4 N_o}\int F_D(\lambda)\varepsilon_A(\lambda)\lambda^4\, d\lambda = \frac{9000(\ln 10)\beta^2\phi_D}{128\pi^5 n^4 N_o} J(\lambda) \tag{6}$$

where n is the refractive index of the solvent, N_o is Avogadro's number, β^2 is the orientation factor equal to 2/3 for isotropic media, λ is the wavelength, $\varepsilon_A(\lambda)$ is the molar decadic extinction coefficient of the acceptor, and $F_D(\lambda)$ is the normalized spectral distribution of the donor (i.e., $\int F_D(\lambda)\, d\lambda = 1$). The values of R_o and $J(\lambda)$ are tabulated in Table 1. As shown in this table, the concentration variation of the acceptor molecules in the D/A pair has limited influence in estimating the critical distance [28]. The average value of R_o was 53 Å, which suggests that the dominant mechanism responsible for the energy transfer is the long-range dipole–dipole energy transfer (Förster type), because the Förster type is usually effective in the range of 10 Å–100 Å [29,30]. Thus, this finding confirmed the appropriateness of the Förster theory to calculate the Förster energy transfer rates as reported by other researchers [31–33].

The R_{DA} was calculated from Equation (5). Fig. 6 shows the influence of the acceptor content on the distance between the donor and acceptor molecules in the presence of TiO_2 NPs. As the acceptor content increased from 0.1 to 5 wt%, the R_{DA} decreased from 65.4 Å to 30.0 Å. This means that the distance between the monomers of PFO and molecules of Fluorol 7GA becomes much smaller in the presence of TiO_2 NPs compared to that in the absence of TiO_2 NPs, which was in the range 42.67 Å–76.20 Å [4].

As shown in Fig. 7, the energy transfer efficiency (η) has an inflection point at $R_{DA} = R_o$. η is close to unity at $R_{DA}<0.5\ R_o$, and it dramatically decreases at $R_{DA} > R_o$. This means that the Förster energy transfer from PFO to Fluorol 7GA in the presence of TiO_2 NPs occurred with a higher probability if the distance between the donor and acceptor molecules was less than 1.5 R_o for 10 Å$<R_o<$ 100 Å, which is in good agreement with previous reports [4,34].

Additional evidence for the efficient energy transfer from PFO to Fluorol 7GA in the presence of TiO_2 NPs can be obtained from the values of energy transfer lifetime (τ_{ET}), energy transfer rate (k_{ET}), and the total decay rate of the donor ($k_{ET} + \tau_D^{-1}$). These parameters are listed in Table 2. They were calculated using the following Equations (7) and (8) [24,35]:

$$k_{ET} = \frac{1}{\tau_D}\left(\frac{R_0}{R_{DA}}\right)^6 \tag{7}$$

$$\tau_{ET} = \frac{1}{[A]k_q} \tag{8}$$

The reduction of τ_{ET}, increase of k_{ET}, and the total decay rate upon an increase in the acceptor content indicate the efficient energy transfer in the current system [24]. On the other hand, without TiO_2 NPs, the values of τ_{ET} are almost two times smaller, whereas the values of k_{ET} and the total decay rate are much larger than those in the presence of TiO_2 NPs [4]. These findings are another evidence

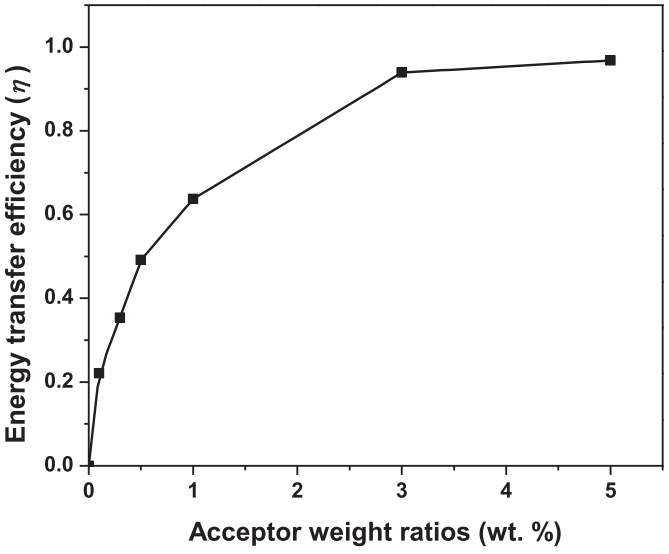

Fig. 5. Efficiency of energy transfer from PFO/TiO_2 to Fluorol 7GA for different weight ratios.

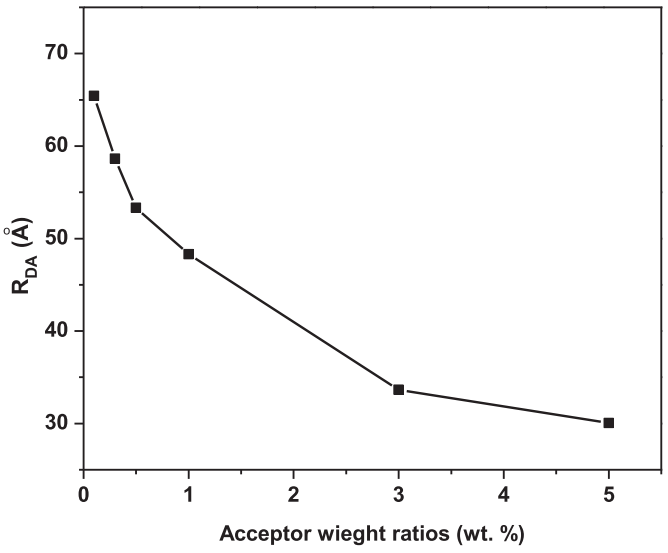

Fig. 6. Distance between donor/acceptor molecules in the presence of TiO_2 versus the acceptor content.

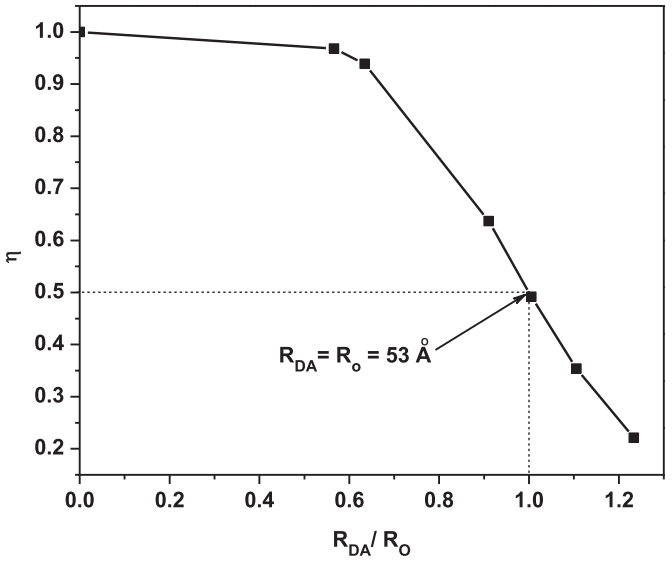

Fig. 7. Dependence of efficiency of energy transfer (η) on the distance between donor/acceptor molecules in the presence of TiO_2.

for the positive effect of TiO_2 NPs on the enhancement of FRET between PFO and Fluorol 7GA.

Fig. 8 demonstrates the influence of the acceptor content on the current density (J) of the PFO/TiO_2 nanocomposite under forward bias (V). It can be observed that the current density decreases with increasing acceptor content. This reduction can be attributed to the resistivity improvement of the light emitting layer [36]. Furthermore, the decrease in the current density of the devices means an increase in the hole-electron pair (exciton) confinement and exciton recombination efficiency, which are essential for the enhancement of the device performance [37,38]. The energy transfer can occur together with the charge trapping process in the ITO/(PFO/TiO_2)/Fluorol 7GA/Al devices as evidenced by the J–V behavior (Fig. 8). Moreover, it can be clearly seen that the turn-on voltage decreased faster upon an increase in the Fluorol 7GA content in the presence of TiO_2 NPs [4], which provides the evidence of the important role of the existing TiO_2 NPs in enhancing the OLED performance.

A broad visible emission of the EL spectra extending from 400 nm up to 750 nm for all devices is demonstrated in Fig. 9. The EL spectra of PFO/TiO_2 (Fig. 9(a)) exhibited two green emission peaks at 519 and 555 nm in addition to two blue emission peaks at 425 and 450 nm. The two green emission peaks are related to the electrochemical degradation of PFO and keto defect during the device operation and fabrication, respectively [5,39], while the blue emission peaks can be attributed to PFO [5]. A new shoulder peak at 590 nm was detected in addition to the previously observed PFO/TiO_2 peaks upon addition of Fluorol 7GA. These findings can be

Table 2
Energy transfer rate, energy transfer lifetime and total decay rate of (PFO/TiO_2)/Fluorol 7GA nanocomposite.

Acceptor content in (donor/TiO_2)/acceptor blend	k_{ET} $(ns)^{-1}$	τ_{ET} (ps)	Total decay rate $(ns)^{-1}$
0.1 wt %	0.821	517	3.71
0.3 wt %	1.58	173	4.47
0.5 wt %	2.79	103	5.68
1.0 wt %	5.07	51.7	7.96
3.0 wt %	44.4	17.3	47.3
5.0 wt %	87.6	10.3	90.4

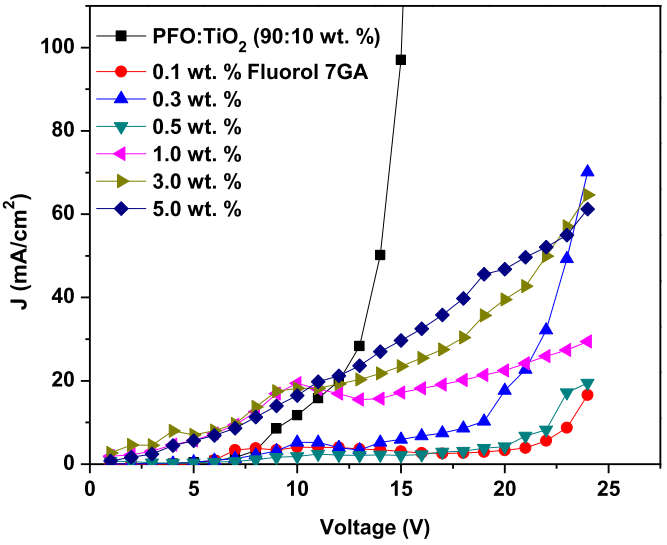

Fig. 8. J–V characteristics of PFO/TiO_2 and (PFO/TiO_2)/Fluorol 7GA OLED devices.

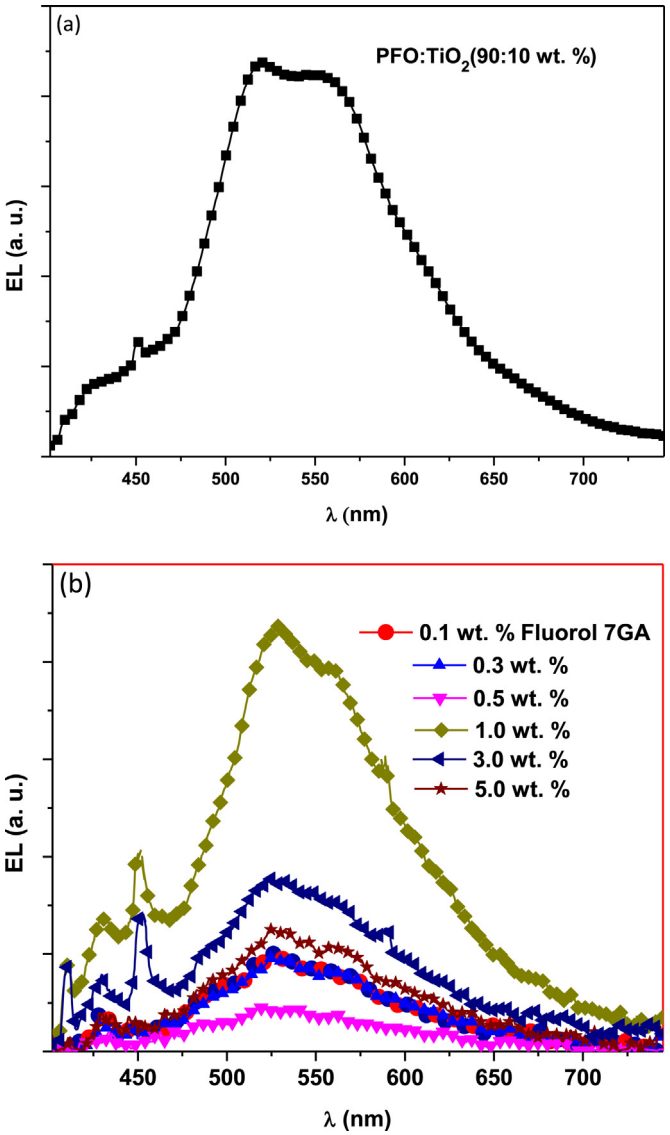

Fig. 9. Electroluminescence spectra of (a): PFO/TiO_2 and (b): (PFO/TiO_2)/Fluorol 7GA OLED devices.

attributed to the carrier trapping processes and Förster-type energy transfer, which can manifest together in the device. The optimum weight ratio of Fluorol 7GA was 1.0 wt % based on the EL measurements (Fig. 9(b)), which is consistent with the PL measurements (Fig. 2).

4. Conclusion

Optoelectronic properties and Förster energy transfer of PFO/Fluorol 7GA hybrid thin films in the presence of TiO_2 NPs have been investigated. The strong overlap between the emission band of PFO and the absorption band of Fluorol 7GA in the presence of TiO_2 NPs was crucial for an efficient energy transfer in the (PFO/TiO_2)/Fluorol 7GA blend. PFO intensity quenching in the presence of TiO_2 NPs and an enhancement in the intensity of Fluorol 7GA indicated an efficient nonradiative energy transfer from the donor to the acceptor. The large values of R_o, k_{SV}, and k_{ET} indicate that FRET is the dominant mechanism for energy transfer. Both the Förster energy transfer and trapping process in the ITO/(PFO/TiO_2)/Fluorol7GA)/Al led to an improvement in the OLED performance. Further improvement of the device performance can be expected by incorporating the emissive layer ((PFO/TiO_2)/Fluorol7GA) in between an appropriate hole and electron transport layers, which will be studied in detail in the future.

Acknowledgments

This project was supported by King Saud University, Deanship of Scientific Research, College of Science Research Center.

References

[1] L.-J. Fan, W.E. Jones Jr., Energy Transfer and Electronic Energy Migration Processes, in: Photochemistry and Photophysics of Polymeric Materials, John Wiley & Sons, Inc., 2010, pp. 1–39.
[2] F. Reil, U. Hohenester, J.R. Krenn, A. Leitner, Förster-type resonant energy transfer influenced by metal nanoparticles, Nano Lett. 8 (2008) 4128–4133.
[3] B.A. Al-Asbahi, M.H.H. Jumali, C.C. Yap, M.M. Salleh, M.S. AlSalhi, Inhibition of dark quenching by TiO2 nanoparticles content in novel PFO/Fluorol 7GA hybrid: a new role to improve OLED performance, Chem. Phys. Lett. 570 (2013) 109–112.
[4] B.A. Al-Asbahi, M.H.H. Jumali, C.C. Yap, M.H. Flaifel, M.M. Salleh, Photophysical properties and energy transfer mechanism of PFO/Fluorol 7GA hybrid thin films, J. Lumin. 142 (2013) 57–65.
[5] B.A. Al-Asbahi, H. Jumali, M. Hafizuddin, C.C. Yap, M.M. Salleh, Enhancement of Poly (9, 9'-di-n-octylfluorenyl-2.7-diyl) Optoelectronic Properties in Novel Conjugated Polymer/Laser Dye Hybrid OLEDs, Mater. Sci. Forum 756 (2013) 281–288.
[6] C. Zhang, H. Von Seggern, K. Pakbaz, B. Kraabel, H.W. Schmidt, A.J. Heeger, Blue electroluminescent diodes utilizing blends of poly (p-phenylphenylene vinylene) in poly (9-vinylcarbazole), Synth. Met. 62 (1994) 35–40.
[7] N. Sharma, S. Kumar, Y. Chandrasekaran, S. Patil, Maleimide–based donor-π-acceptor-π-donor derivative for efficient organic light-emitting diodes, Org. Electron. 38 (2016) 180–185.
[8] T. Chao, L. Feng, X. Hui, H. Wei, Polyfluorene and its derivatives as electroluminescent materials, Prog. Chem. 19 (2007) 1553.
[9] Q. Pei, Y. Yang, Efficient photoluminescence and electroluminescence from a soluble polyfluorene, J. Am. Chem. Soc. 118 (1996) 7416–7417.
[10] A.R. Buckley, M.D. Rahn, J. Hill, J. Cabanillas-Gonzalez, A.M. Fox, D.D.C. Bradley, Energy transfer dynamics in polyfluorene-based polymer blends, Chem. Phys. Lett. 339 (2001) 331–336.
[11] A. Danel, Ł. Chacaga, T. Uchacz, M. Pokladko-Kowar, E. Gondek, P. Karasiński, B. Sahraoui, Solution processable double layer organic light emitting diodes (OLEDs) based on 6-N, N-arylsubstituted-1 H-pyrazolo [3, 4-b] quinolines, Adv. Device Mater. 1 (2015) 17–22.
[12] B.A. Al-Asbahi, M.S. Alsalhi, A.S. Al-Dwayyan, M.H. Haji Jumali, Förster-type energy transfer mechanism in PF2/6 to MEH-PPV conjugated polymers, J. Lumin. 132 (2012) 386–390.
[13] R.J. Nedumpara, P. Manu, C. Vallabhan, V. Nampoori, P. Radhakrishnan, Energy transfer studies in dye mixtures in different solvent environments, Opt. Laser Technol. 40 (2008) 953–957.
[14] A. Bacher, C.H. Erdelen, W. Paulus, H. Ringsdorf, H.-W. Schmidt, P. Schuhmacher, Photo-cross-linked triphenylenes as novel insoluble hole transport materials in organic LEDs, Macromolecules 32 (1999) 4551–4557.
[15] C. Yin, T. Kietzke, D. Neher, H.H. Hörhold, Photovoltaic properties and exciplex emission of polyphenylenevinylene-based blend solar cells, Appl. Phys. Lett. 90 (2007) 092117.
[16] L.-G. Yang, P. Wu, X. Liu, P.-F. Gu, M. Wang, H.-Z. Chen, Electric field evolution of charge and energy transfer in molecule-doped polymer light-emitting diodes, Mater. Chem. Phys. 114 (2009) 660–664.
[17] M.S. Alsalhi, Z.S. Abu Mustafa, V. Masilamani, External energy transfer in amplified spontaneous emissions from MEH-PPV conjugated polymer, Opt. Laser Technol. 43 (2011) 147–151.
[18] T. Virgili, D.G. Lidzey, D.D.C. Bradley, Efficient energy transfer from blue to red in tetraphenylporphyrin-doped poly(9,9-dioctylfluorene) light-emitting diodes, Adv. Mater. 12 (2000) 58–62.
[19] N. Sesha Bamini, A. Ramalingam, V.S. Gowri, Comparative photophysical and energy transfer studies of C480:C535 binary dye mixture in solid and liquid environments, J. Lumin. 130 (2010) 1011–1020.
[20] K.K. Pandey, T.C. Pant, Migration modulated donor-acceptor energy transfer in PMMA, J. Lumin. 47 (1991) 319–325.
[21] J. Liu, Y. Shi, Y. Yang, Improving the performance of polymer light-emitting diodes using polymer solid solutions, Appl. Phys. Lett. 79 (2001) 578–580.
[22] N.J. Turro, Modern Molecular Photochemistry, University Science Books, 1991.
[23] S. Brown, An Introduction to Spectroscopy for Biochemists, 1980, p. 7. Book Reviews, 25.
[24] J.R. Lakowicz, Principles of Fluorescence Spectroscopy, Springer London, Limited, 2009.
[25] K. Pandey, H. Joshi, T. Pant, Excitation energy migration and transfer in a dye pair in PMMA, J. Lumin. 42 (1988) 197–203.
[26] W.T. Silfvast, Laser Fundamentals, Cambridge University Press, 2004.
[27] A. Gilbert, J.E. Baggott, Essentials of Molecular Photochemistry, CRC, 1991.
[28] J.-W. Yu, J.K. Kim, D.Y. Kim, C. Kim, N.W. Song, D. Kim, Prediction of efficient energy transfer in emissive polymer blends based on Förster radius and the excited state lifetime of acceptors, Curr. Appl. Phys. 6 (2006) 59–65.
[29] B.J. Schwartz, Conjugated polymers as molecular materials: how chain conformation and film morphology influence energy transfer and interchain interactions, Annu. Rev. Phys. Chem. 54 (2003) 141–172.
[30] P. Wu, L. Brand, Resonance energy transfer: methods and applications, Anal. Biochem. 218 (1994) 1–13.
[31] F. Kong, J. Liu, X. Zhang, Y. An, X. Li, B. Lin, T. Qiu, Effect of distance between acceptor and donor on optical properties of composite semiconducting polymer films, J. Lumin. 131 (2011) 815–819.
[32] A. Mallick, B. Haldar, S. Sengupta, N. Chattopadhyay, 7-Hydroxy-4-methyl-8-(4′-methylpiperazine-1′-yl)methyl coumarin: an efficient probe for fluorescence resonance energy transfer to a bioactive indoloquinolizine system, J. Lumin. 118 (2006) 165–172.
[33] U. Mote, S. Patil, S. Bhosale, S. Han, G. Kolekar, Fluorescence resonance energy transfer from tryptophan to folic acid in micellar media and deionised water, J. Photochem. Photobiol. B 103 (2011) 16–21.
[34] B. Valeur, M.N. Berberan-Santos, Molecular Fluorescence: Principles and Applications, John Wiley & Sons, 2012.
[35] T. Förster, Fluoreszenz organischer verbindungen, Vandenhoeck & Ruprecht Göttingen, 1951.
[36] R.-H. Lee, H.-H. Lai, Enhancing electroluminescence performance of MEH-PPV based polymer light emitting device via blending with organosoluble polyhedral oligomeric silsesquioxanes, Eur. Polym. J. 43 (2007) 715–724.
[37] Q. Zhang, D.K. Chambers, S. Selmic, Polymer Light-Emitting Diodes Based on Poly [9, 9-di-(2′-ethylhexyl) fluorenyl-2, 7-diyl], J. Nanoelectron. Optoelectron. 1 (2006) 219–223.
[38] S.-N. Hsieh, T.-Y. Kuo, P.-C. Hsu, T.-C. Wen, T.-F. Guo, Study of polymer blends on polymer light-emitting diodes, Mater. Chem. Phys. 106 (2007) 70–73.
[39] S. Zaman, A. Zainelabdin, G. Amin, O. Nur, M. Willander, Influence of the polymer concentration on the electroluminescence of ZnO nanorod/polymer hybrid light emitting diodes, J. Appl. Phys. 112 (2012) 064324.